ISSN 0145-8752, Moscow University Geology Bulletin, 2021, Vol. 76, No. 4, pp. 374–382. © Allerton Press, Inc., 2021.
Russian Text © The Author(s), 2021, published in Vestnik Moskovskogo Universiteta, Seriya 4: Geologiya, 2021, No. 3, pp. 26–34.

The Lithological and Geochemical Characteristics and Paleoclimatic Conditions of Formation of the Turonian–Santonian Sediments of the Epicontinental Basin of the Russian Plate in the Voronezh Anteclise Region

R. R. Gabdullin[a, *], A. Yu. Puzik[b, **], S. I. Merenkova[a, *], I. R. Migranov[a, ****], N. V. Badulina[a, *****], and M. D. Kazurov[a, ******]**

[a] *Department of Geology, Moscow State University, Moscow, 119991 Russia*
[b] *Natural Science Institute, Perm State University, Perm, 614990 Russia*
**e-mail: mosgorsun@rambler.ru*
***e-mail: alex.puzik@mail.ru*
****e-mail: koshelevasof@mail.ru*
*****e-mail: iskandermig@mail.ru*
******e-mail: nvbadulina@mail.ru*
*******e-mail: max.kazurov@yandex.ru*

Received December 8, 2020; revised January 28, 2021; accepted January 29, 2021

Abstract—We present the results of a geochemical study and their paleogeographic and paleoclimatic interpretation for a cyclically constructed section of the Upper Cretaceous deposits near Staryi Oskol in the Belgorod region.

Keywords: Cretaceous period, cyclicity, geochemistry, climate system, Stary Oskol

DOI: 10.3103/S0145875221040037

INTRODUCTION

Phanerozoic sediments of the cover of the East European platform were exposed in the section of the open pit of the Stoilensky mining and processing plant (SMPP) of the Kursk magnetic anomaly in the city of Stary Oskol (Belgorod region). The Upper Cretaceous part of the section includes terrigenous formations of the Cenomanian and carbonate formations of the Turonian–Lower Santonian.

Earlier (Gabdullin, 2002; Gabdullin and Ivanov, 2002) this section was studied using a set of methods. The key factors that generated cyclicity in the Turonian–Early Antonian time were identified, that is, the cycles of bioproductivity associated with climate variations, in turn, caused by cycles of the eccentricity of the second (lasting approximately 400000 years) and the fourth (lasting approximately 2030000 years) order. This is confirmed by the distribution of the number of ichnotaxons, the area (volume) of bioturbation, the contents of organic carbon (C_{org}) and calcium carbonate ($CaCO_3$), destruction of the fields of remanent saturation magnetization, as well as natural remanent magnetization and remanent saturation magnetization.

Data on changes in the temperature, depth, salinity, and climate type are given for the entire interval of the Upper Cretaceous part of the section. In addition, curves of these parameters are plotted. Such data for this section have not been previously published. They are interesting from the standpoint of reconstructing the climate and paleogeographic history of the development of the epicontinental seas that covered the Russian Plate in the Voronezh anteclise area.

MATERIALS AND METHODS

The geological section was studied using a complex of methods. A review of the results of these studies and their interpretation was published earlier in (Gabdullin, 2002; Gabdullin and Ivanov, 2002).

The emphasis in our work is made on the results of geochemical studies of the section using rock samples collected by R.R. Gabdullin and their paleogeographic and paleoclimatic interpretation.

A complete geochemical analysis of the 47 samples of Turonian, Coniacian, and Santonian deposits from a cyclically constructed section was carried out on a sequential S8 Tiger wave-dispersive X-ray fluorescence spectrometer (Bruker), analyst A.Yu. Puzik.

Based on the results we obtained, the ratios and values of the content of some chemical elements were

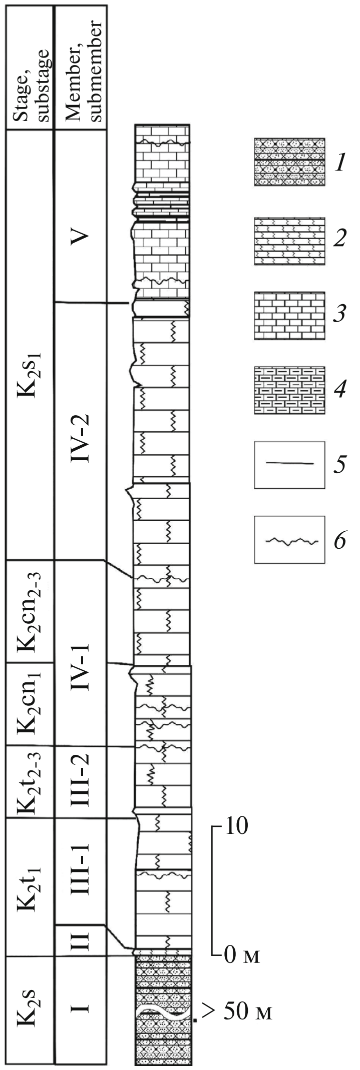

Fig. 1. Section of the Upper Cretaceous deposits of the quarry of Stoilensky MPP, Staryi Oskol, Belgorod region: *1*, sandstones; *2*, writing chalk; *3*, limestone; *4*, clayey limestones (marls); *5*, consonant stratigraphic boundaries; *6*, discordant stratigraphic boundaries

determined, indicating a change in the conditions of sedimentation (basin depth, hydrodynamics, climate, etc.), which made it possible to clarify the previously formulated ideas about the sedimentation regime. Let us briefly characterize these parameters, which were previously described in detail in several works (Badulina et al., 2016; Gabdullin et al., 2021; Merenkova et al., 2020; etc.).

The following values of the element concentrations and their ratios were used to analyze *variations in paleotemperature values*: V, Ca, Ni, Ca/Sr, titanium modulus (TM), Mn, Si/Al, Ca/Mg, Sr/Ba, Zn/Nb, and (Ce, Nd, La, and Ba)/Yb (Y and Zr). An increase in the concentrations of Ca, Sr, and Mg may indicate an arid type of climate, and an increase in the contents of Sc, Ni, Zn, Y, W, U, Cu, V, and rare earth elements (REE) may indicate humid sedimentation conditions (*Climate*..., 2004; Engalychev and Panova, 2011).

The indicators of changes in the depth of the basin include the ratio Fe/Mn, Ti/Mn, the titanium modulus (TM), the sodium modulus (NM), and the potassium modulus (KM), as well as the elements Zn, Pb, Al, Mn, Cu, Sr, and Ba, indicating the displacement of facies (Badulina et al., 2016; Gabdullin et al., 2021; Merenkova et al., 2020).

The values of the Sr/Ba and Ca/Sr ratios were used for the analysis of *the salinity variations*. Their increase indicates an increase in the salinity of the solution. The concentrations of B, Ba, S, Cr, Cu, Ga, Ni, and V in marine sediments are higher than in freshwater, and the contents of Zn and Cu in marine sediments are lower than in freshwater (Badulina et al., 2016; Gabdullin et al., 2021; Merenkova et al., 2020).

Determination of paleotemperature by the weathering index. Weathering indices usually show the degree of depletion of rocks by mobile elements relative to immobile ones during chemical weathering. The CIA index (Nesbitt and Young, 1982) is widely used as an indicator of the intensity of chemical weathering

$$CIA = 100Al_2O_3/(Al_2O_3 + CaO^* + Na_2O + K_2O),$$

where CaO* is noncarbonate CaO and all variables represent the molar amounts of oxides of the main elements.

$$T = 0.56CIA - 25.7\ (r^2 = 0.50),$$

where T is the temperature, °C. A detailed description of the method was reported in (Merenkova et al, 2020; Gabdullin et al., 2021).

The lithological and paleontological characteristics of the section. The section (Fig. 1) is in the northwestern side of the open pit of the Stoilensky GOK, KMA in the town of Staryi Oskol (Belgorod region). The section was described and studied in (Gabdullin, 2002; Gabdullin and Ivanov, 2002).

Cenomanian stage. Lower and middle (?) substages. Member I. Greenish-grayish, brown, medium-grained, glauconite sands. Sandstones are brown, ferruginous, dense. The member contains two or three horizons of phosphorite nodules.

Macrofossils are represented by bivalve mollusks, including oysters, forming banks; an abundance of remains of shark, chimera and teleost fishes, belemnite rostras, rare ammonites. Fossilized tree trunks of the genus *Cupresssinoxylon* and coprolites of large marine reptiles are found. The member is up to 50-m thick (Gabdullin, 2002).

The section of Cenomanian deposits is dominated by a member of rhythmic interbedding of gray, gray-green sandstones with brown ferruginous dense sandstones (7–8 m). Macrofauna: teeth of chimeras *Ischyodus* "*bifurcatus*" Case and sharks *Protosquales* sp.; shells of *Neithea* sp.; rostra *Praeactinocamax primus* Arkh. The microfauna is represented by Cenomanian–Maastrichtian forms of calcareous nanoplankton

Manivitella redimiculata (Stover), *Prediscosphaera cretacea* (Arb.) and Cenomanturonian *Broisonia matalosa* (Stover), etc. These deposits are underlain by lenticular interlayers of clay and clayey sands (0–2.5 m) with phosphorites, which lie above the Cenomanian–Turonian boundary. Below this level lies a member of Upper Albian sands and sandstones, where *Mortoniceras inflatum* was found by one of the authors. Thus, the boundary between the Upper Albian and the Lower Cenomanian runs along the base of lenticular sands with phosphorites (Gabdullin, 2002).

The member is cyclical (four cyclites of dense sandstone (0.2–0.3 m), sand, and sandstone (0.5–0.7 m).

The Turonian Stage. Lower substage, members II and III

Member II (0.7–1-m thick), "surka." Sandy chalk with evenly dispersed phosphorite nodules and horizons of fragments of the Inoceram prismatic layer. At the base of the member there is a "phosphorite slab" (its thickness is 0.2 m), a highly condensed interlayer of cemented phosphorite nodules of various shapes and degrees of roundness, black and brown, with glauconite. The Turonian age of the "surka" in this section is confirmed by the occurrence of the calcisphere *Broisonia matalosa* (Stover), *Br. parca* (Strad.), *Zygodiscus chelmiensis* (Gor.), *Prediscosphaera spinosa* (Bramlette et Martini), coexisting in the Turonian. Macrofossils are represented by oyster shells, goblets of sponges of the genus *Ventriculites*, rounded shark teeth and vertebrae. Cyclicity has not been established (Gabdullin, 2002).

Member III. Writing chalk is white, light gray, yellowish grayish. The member contains numerous macrofossils: belemnites, inocerams, brachiopods, sea urchins, shark teeth, fish scales, coprolites, and ichnofossils. In the lower part (submember III-1), corresponding to the Lower Turonian, two bentonite interlayers and carapaces (Voronezh anteclise) are noted (Gabdullin, 2002).

Submember III-1. Writing chalk (13 m) with two bentonite interlayers and three erosion surfaces. The second interlayer marks the boundary with the base of the Upper Turonian. Lower Turonian–zone Gavelinella nana. It is possible to distinguish one cyclite chalk, that is, clay and one cyclite chalk, marl, or three cyclites of the chalk–"hard ground" type (Gabdullin, 2002).

Middle and upper substages. Submember III–2

Pure writing chalk without bentonite interlayers, 6.5–7-m thick, with *Inoceramus lamarcki* Park., confirming the presence of Middle Turonian sediments. In terms of the microfauna, this stratum corresponds to the *Gavelinella moniliformis* zone (Middle and Upper Turonian). Three surfaces of the "hard bottom" type (shell) have been identified. Cyclicity is represented by interlayering of layers of dense and loose chalk. Thickness of the dense chalk layers of is always 2–3 times less than the thickness of loose chalk layers and is (0.4–0.5 m) (Gabdullin, 2002).

Member III contains a rich fauna complex: bivalves *Dianchora spinosa* (Sow.), oysters "*Ostrea*" sp., Pectenids, sea urchins, sharks *Cretoxyrhina* sp. Traces of *Teichichnus* and *Planolites* were found. The Lower Turonian deposits contain two stratal cyclites, while the Middle and Upper Turonian deposits contain one cyclite (Gabdullin, 2002).

Coniacian Stage. Writing chalk of member IV corresponds in section to the lower and upper Coniacian (submember IV–1), as well as to the lower Santonian (bed IV-2). The division of this member into subunits is based not so much on lithological as on biostratigraphic criteria (Gabdullin, 2002).

Submember IV–1. Writing chalk, microscopically fine-grained limestone. The section shows the deposits of the lower and upper substage. Lower Coniacian deposits (*Gavelinella kelleri* zone) are filled with writing chalk (6.5 m) with one erosion surface. The erosional contact and the overlying horizon of the debris of the inoceramus prismatic layer mark the unconformable boundary of the lower and upper Coniacian. The upper Coniacian (*Gavelinella thalmanni* zone) is represented by writing chalk (9 m). This is where *Volviceramus involutus* Sow was found. (Gabdullin, 2002).

The following complex of macrofauna was found: spatangoid urchins *Micraster rogalae* Nowak, cydaroid hedgehogs, oysters of the genus *Ostrea*. Traces of the *Thallassinoides*, *Teichichnus*, and *Planolites* were found in the Coniacian deposits of the SMPP (Gabdullin, 2002).

Cyclicity was established only in the rocks of the upper Coniacian: one cyclite of the dense chalk (1 m)–loose chalk (5.5 m) (Gabdullin, 2002).

Santonian Stage Lower substage. Carbonate rocks are represented in the lower part by writing chalk (submember IV–2), and in the upper part, by marls and limestones (member V). They lie conformably on the underlying Lower Santonian deposits (*Gavelinella infrasantonica* zone). Finds of *Sphenoceramus cardissoides* (Goldf.) were noted, which also confirms the presence of Lower Santonian deposits (Gabdullin, 2002).

Submember IV–2. Writing chalk is microscopically fine-grained limestone. At the base of the bed, five horizons of fragments of the Inoceram prismatic layer were observed. The thickness of the interlayers is up to 10 cm; the interval is 30–50 cm. An erosion surface is noted at the top of the bed several decimeters before the boundary with member V. The bed is 21-m thick (Gabdullin, 2002).

Member V of the rhythmic interbedding of white fine-grained limestones and marls 10-m thick. In the upper part of the member, there is a break surface. Ichnofossils of the *Thallassinoides*, *Teichichnus*, *Chondrites*, *Zoophycos*, and *Planolites* were identified there (Gabdullin, 2002).

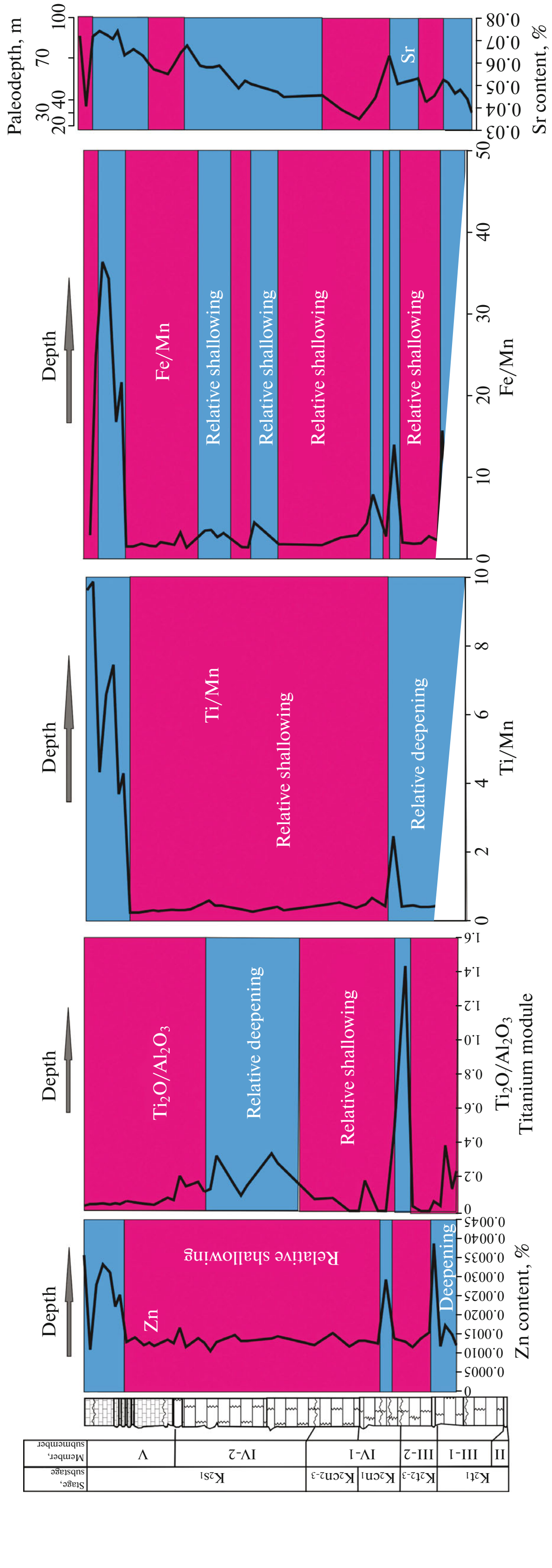

Fig. 2. The ratio of the paleobatimetry curves for the Turonian–Early Santonian time for the Voronezh anteclise, as obtained from geochemical data.

There are two types of cyclicity in the Lower Santonian sediments. Submember IV–2 contains two cyclites. The member of alternating chalk-like marls and limestones contains four cyclites: chalk-like marl (0.3–0.5 m)–limestone (0.6–0.75 m). The cyclicity is well emphasized by the weathering profile (Gabdullin, 2002).

RESULTS AND DISCUSSION

The geochemical characteristics of the section. The geochemical data allowed us to calculate the values of the 29 elements and compound concentrations (ppm), as well as six of their ratios (modules), which are necessary to clarify the conditions of sedimentation and the genesis of the cyclicity of the carbonate part of the section starting from member II. A description of this technique is presented in several works (*Climate*..., 2004; Engalychev and Panova, 2011; Sklyarov, 2001). Our data in the context of paleogeographic interpretation are contradictory and require comparison with the results of other studies. Let us briefly and selectively characterize the elements, compounds, and their concentration ratios.

Variations in the paleo-depth (Fig. 2) are visible on the curves of the concentrations of Zn, Sr, and the titanium modulus (TM). Curves of the Zn and TM contents show the mean correlation. At the same time, they show a weak correlation with the Sr content. The distribution of Ti/Mn and Fe/Mn shows a good correlation with each other and with the distribution of the Zn content. The epochs of relative shallowing and deepening of the basin are recorded on the graphs of all parameters.

According to the distribution of these parameters, four eustatic cycles can be distinguished: the first, in the Turonian, the second, in the Coniacian, the third and the fourth, in the Santonian time. The cycles begin with the transgressive epoch (deepening, transgressive system of tracts), followed by the epoch of depth stabilization (the first half of the high-standing tract), and after it, the regressive epoch (the second half of the high-standing tract).

A correlation was established between a decrease in paleo-depth (under regression conditions) and an increase in a number of parameters determined earlier (Gabdullin, 2002; Gabdullin and Ivanov, 2002): C_{org} concentrations and the ichnofossil distribution (the number of ichnotaxons, the maximum diameters of holes, and the area (volume) of bioturbation along the section). In particular, the Zn content correlates well with the ichnofossil distribution, except for the lower part of Member V (early Early Santonian), in contrast to the Sr concentration. TM variations correlate well with the S_{org} content and the ichnofossils distribution, while the Sr content variations are best correlated with the fossil distribution. The weak correlation of Sr with the ichnofossil distribution over the section can be explained by the variations in the gas regime in the bottom waters and/or in the salinity and depth. The transformation of the Sr content curve into a paleobatimetric curve with a depth scale was carried out considering the data of the paleoecology of fossil organisms, that is, the indicators of a complex system (paleoenvironment).

In the Turonian, the paleodepth of the basin is estimated at 40–100 m, approximately 40–50 m in the Early Turonian, and as the transgression develops, up to 100 m in the second half of the Turonian. One relatively shallow eustatic cycle corresponds to this interval of the section. The paleocenosis was dominated by plankton with carbonate skeletons, benthic forms of animals (pelecypods and brachiopods) over nekton types (belemnites, sharks (*Cretoxyrhina* sp.) and bony fishes). The presence of the sponges *Ventriculites* indicates a comparatively great depth: several hundred meters to several kilometers. Occurence of cidaroid urchins usually indicates a depth of 75–100 m. Numerous oysters, including the genus Ostrea, usually live no deeper than 40–100 m. Cidaroid urchins feed on sea sponges, respectively, these organisms coexisted together at a depth of more than 80–100 m (sublittoral and pelagial). The shallowest representatives of this community are pectenids (10–50 m) and oysters —pycnodonts (30–40 m) (Gabdullin, 2002).

For the Coniacian time, the paleodepth of the basin is also estimated in the range of 40–100 m. This interval of the section corresponds to one eustatic cycle at approximately 40–50 m in the early Coniacian and with the development of transgression up to 100 m in the second half of the Coniacian age. The paleocenosis contains plankton with a carbonate skeleton, as well as crustaceans (traces of *Thallassinoides*), inocerams, and sea urchins. No nekton forms of macrofauna was found. The foraminiferal assemblage is represented by anomalines (Gabdullin, 2002).

In the Early Santonian, the paleodepth range did not exceed 100 m, and by the end of the Early Santonian it decreased. Two eustatic cycles correspond to this range of the section. The paleocenosis includes plankton with a carbonate skeleton, benthic forms were inocerams and nekton forms were belemnites and bony fishes. The microfossils include the shells of the foraminifera *Trochammina borealis* Keller, which usually inhabit the middle shelf (60–100 m, sublittoral). Towards the end of the early Santonian the depth of the basin decreased. This is indicated by the change of the writing chalk facies to the limestone-marl facies (Gabdullin, 2002).

Variations in the paleotemperature values were established by the contents of V, Cu, Ni, Mn, and the Si/Al ratio (Fig. 3), which correlate with each other in different ways. For the curve of paleotemperature variation, the curve of the Cu content was chosen, as it most closely correlates with the distribution of ichnofossils. In particular, the Cu concentration in the

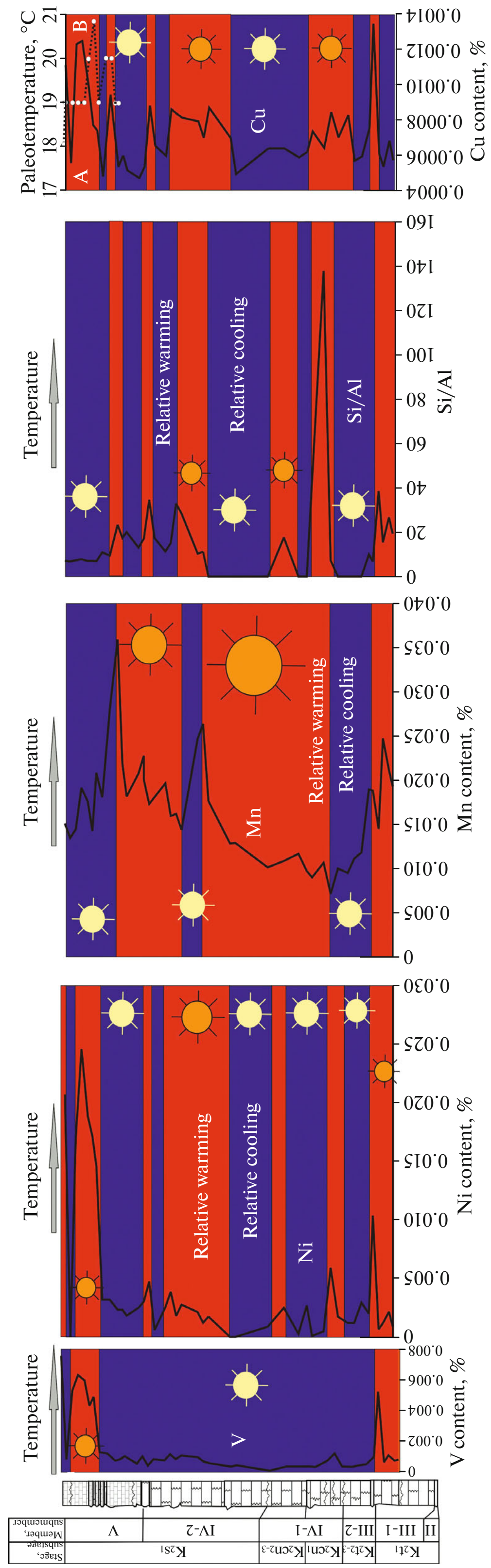

Fig. 3. The variations in paleotemperature for the Turonian–Early Santonian time for the Voronezh anteclise, obtained from geochemical data: (A) paleotemperature curve (based on Cu content); B, paleotemperature curve for the Early Santonian time (calculated from the weathering indices).

Table 1. The calculated paleotemperature based on the weathering index

Serial number	Sample number	Sample	CIA	T, °C
1	X10818	Oscol 62	80	19
2	X10819	Oscol 63	80	19
3	X10820	Oscol 64	81	20
4	X10821	Oscol 65	81	20
5	X10822	Oscol 66	80	19
6	X10823	Oscol 67	83	21
7	X10824	Oscol 68	81	20
8	X10825	Oscol 71	79	19
9	X10826	Oscol 72	79	19
10	X10827	Oscol 73	79	19
11	X10828	Oscol 74	79	19
12	X10829	Oscol 76	78	18

In the studied sediments, to calculate the CIA and paleotemperature values, we used the samples with the highest amount of terrigenous admixture. The content of SiO_2 > 5% and Al_2O_3 > 1% was taken as a criterion.

epochs of relative warming are well correlated with an increase in the number of ichnotaxons, the diameters of the holes, and the area (volume) of bioturbation, and simultaneously with a decrease in the C_{org} content. It became possible to move from a "qualitative" graph to a curve with quantitative values based on the results of determining the values of paleotemperature by the weathering index (Table 1), calculated for the Lower Santonian deposits. The obtained paleotemperature range of the Earth's surface of 18–21°C on paleo-uplifts (in the areas of denudation) can be approximated with the temperature of the water surface and the upper shallow layers of the water column, since the temperature decreases with depth (up to 100 m). This is indirectly confirmed by the presence of heat-loving amphidonts, ostry, and pectenids in the fossil community of the Turonian, which allows us to conclude that the basin was warm (Fig. 3); therefore, the range of values 18–21°C was chosen for the paleotemperature scale.

The range of 18–21°C is "warmer" than the values previously obtained by isotope paleothermometry for nektonic forms (belemnites) (Teis and Naidin, 1973) for the comparatively deeper parts of the epicontinental basins of the Russian Plate in the second half of the Turonian (14–15°C) or the second half Coniacian (13–15°C) (Gabdullin, 2002).

Six climatic cycles can be distinguished, starting with the cooling phase. The first one was in the Early Turonian time (submember III-1), the second was in

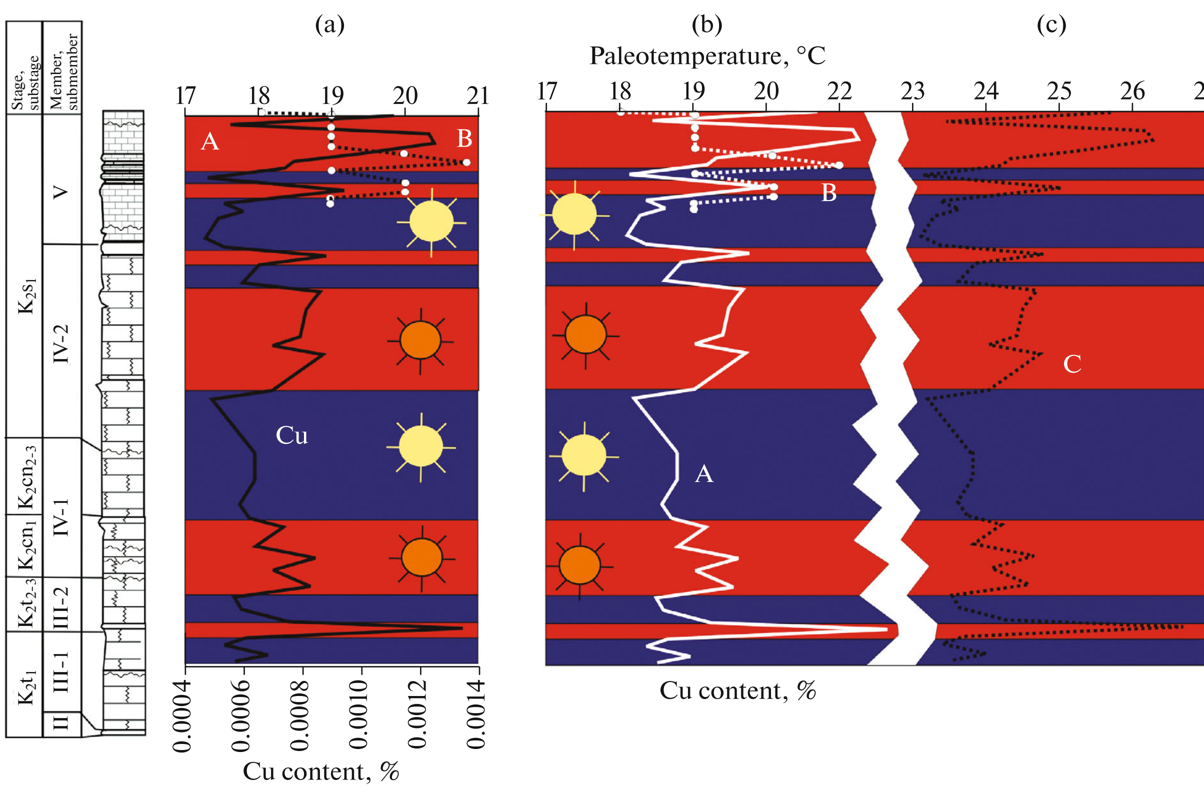

Fig. 4. The paleotemperature curves for the Turonian–Early Santonian time: (a) corrected paleotemperature curve for land (analogous to the average annual temperature (in terms of Cu content)) taking the values of paleotemperatures for oysters into account; (b) the same, adjusted for the values of paleotemperatures obtained from the weathering indices; (c) (C), the assumed paleotemperature curve for the surface waters of the sea basin; A, corrected paleotemperature curve (by Cu content); B, paleotemperature curve for the Early Santonian time (calculated from the weathering indices).

the Late Turonian–Early Coniacian time (submember III-2 and the lower half of submemmber IV-1). The third cycle covers the time from the middle Coniacian to the beginning of the Early Santonian (top of IV-1 and bottom of IV-2). The fourth, fifth, and sixth cycles include the interval of the section that corresponds to the top of submember IV-2 and member V. Thus, the times of relative warming tend to the boundaries of the members (although they may also be inside them): the end of the Early Turonian (18–21°C), late Turonian–early Coniacian (18–19°C), and three warming phases in the early Santonian (18.5–21°C). The time of relative cooling was the end of the Early Turonian and the Middle Turonian (17.5–18.5°C), the middle Coniacian–early Santonian (17.5–18°C), as well as three more episodes of cooling in the Early Santonian (17.5–18°C).

The Cu content curve, taken as a paleotemperature curve (curve "A") and corrected for the values of paleotemperature inhabited by the fossil organisms, is similar to the curve of paleotemperature values calculated from the weathering indices (curve B, Fig. 3). Taking the paleotemperature values according to the weathering indices into account (which are approximately 1°C higher), the position of the paleotemperature curve was corrected; the graph was shifted towards higher values (Fig. 4) by approximately 1°C (curve B), i.e., paleotemperature values were corrected for six climatic cycles. Relatively warmer epochs were the end of the Early Turonian (19–22°C), the Late Turonian–early Coniacian (19–20°C) and three phases of warming in the early Santonian (19–22°C). Relatively colder epochs include the end of the Early Turonian and the Middle Turonian (18.5–19.5°C), the middle Coniacian–early Santonian (18.5–19°C), and three more episodes of cooling in the early Santonian (18.5–19°C).

A surface water paleotemperature curve is proposed (Fig. 4, curve B). Under the conditions of the Late Cretaceous thalassocracy and a high level of ocean standing, the temperature of sea waters is estimated to be approximately 5°C higher than the land temperature (when comparing the mean annual temperature (MAT), the mean annual air temperature (MAAT) (Burgener and Hyland, Huntington et al., 2019) with the sea surface temperature (SST) (O'Brian et al., 2017), for example, for the Campanian Kaiparovich Formation (United States)). These values do not contradict the values of the World Ocean paleotemperature for the basins of temperate paleolatitudes in the Turonian–Early Antonian time, 20–25°C, and a decrease in the global temperature was noted in the indicated time (O'Brian et al., 2017).

Climate humidity variations are traced on the Sr, Mg, V, PM, SM, and TM curves (Fig. 5). The graphs of the modules (PM, SM, and TM) correlate weakly with each other (their individual intervals do not correlate at all). Curves of V, Sr and PM variations

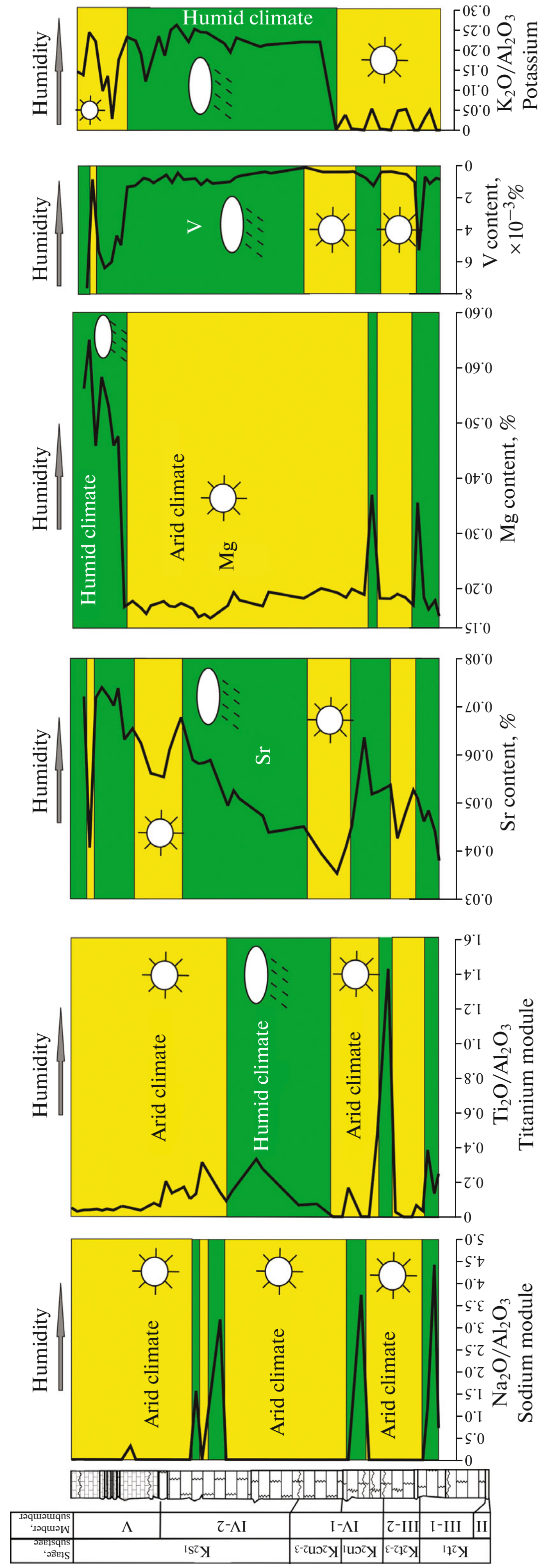

Fig. 5. The change in the type of climate (arid / humid) in the study area for the Turonian–Early Santonian time

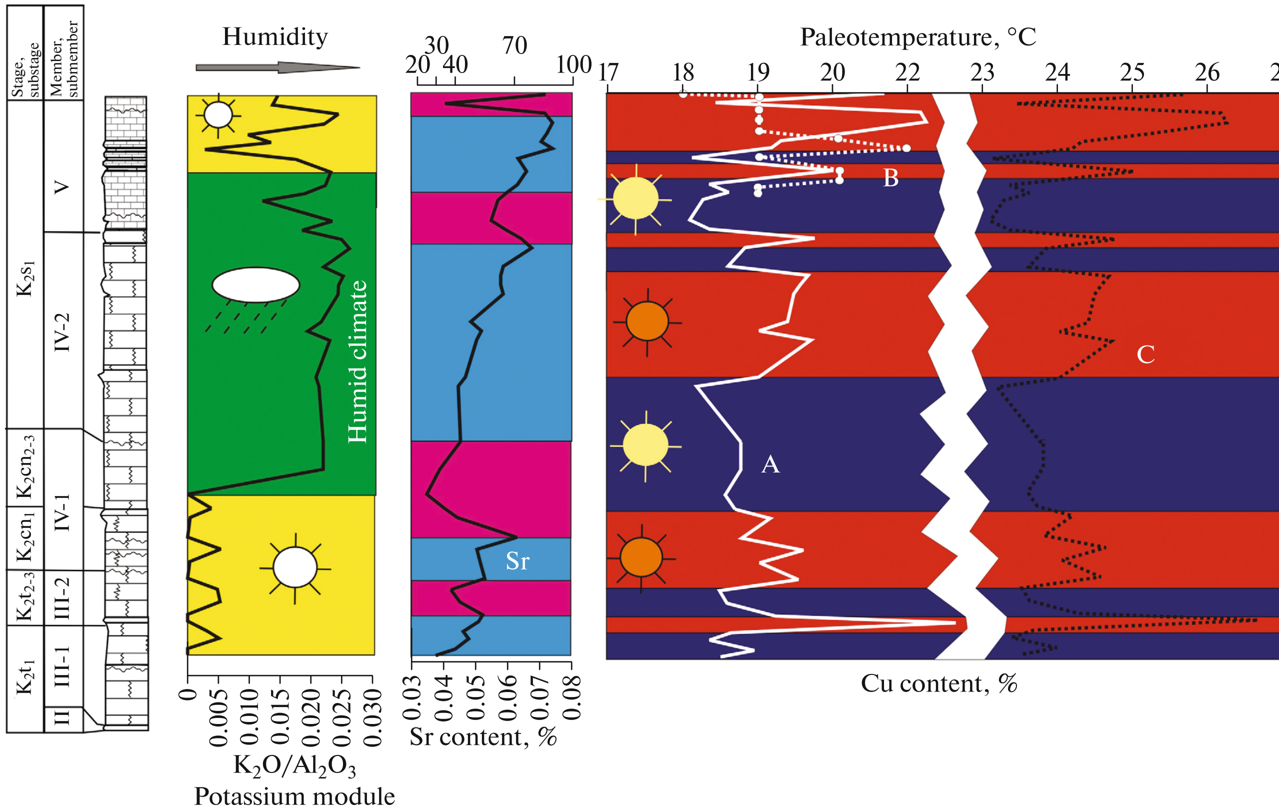

Fig. 6. Variations in paleotemperature for the Turonian–Early Santonian time for the Voronezh anteclise obtained from geochemical data: A, corrected paleotemperature curve for land (analogous to the average annual temperature) taking into account the values obtained from the weathering indices; corrected paleotemperature curve (based on Cu content); B, paleotemperature curve for the Early Santonian time (calculated from weathering indices); C, assumed paleotemperature curve for surface waters of the sea basin

demonstrate the best correlation with each other. PM was chosen as a parameter for assessing climate humidity, which shows a direct correlation with the ichnofossil distributions (area of bioturbated rocks, maximum hole diameter, and number of ichnotaxons), C_{org} content, and the destructive field of the remanent saturation magnetization determined earlier (Gabdullin, 2002). In the era of humidization of the climate in the Turonian–Coniacian time, the content of C_{org} and the destructive field of saturation remanent magnetization increased, more ichnofossils appeared, while in the epoch of aridization it decreased.

As a result, we can distinguish two intervals of relatively humid climate (Turonian–early Coniacian and the second half of Early Santonian, that is, the time of formation of member V) and an interval of an arid climate (middle Coniacian–beginning of the Early Santonian, the time of formation of the second half of submember IV-1 and submember IV-2).

Variations in the paleosalinity values are traced on the Sr/Ba ratio curve, which can be plotted only for fragments of the section. For the end of the Early Santonian, a local decrease in salinity (Sr/Ba ratio) was noted, which correlates with a decrease in the basin depth. The presence of echinoderms (in addition to crustaceans and pelecypods) in the Turonian–Coniacian time and inocerami and cephalopods in the Early Antonian time indicates the normal salinity of the epicontinental sea basin that covered the region of the Voronezh anteclise.

CONCLUSIONS

Variations in temperature, depth, and salinity of the epicontinental basin, as well as climate humidity in the Late Cretaceous (Turonian–Early Santonian) time were analyzed using the example of the section of the Voronezh anteclise, that is, the quarry of the Stoilensky MPP in the city of Stary Oskol (Belgorod region) (Fig. 6).

Four eustatic cycles were identified: the first was in the Turonian, the second was in the Coniacian, and the third and fourth were in the Santonian time. The cycles begin with a transgressive epoch (deepening, transgressive system of tracts), followed by an epoch of depth stabilization (the first half of the high-standing tract), and after it, a regressive epoch (the second half of the high-standing tract).

For the Turonian, the paleodepth of the basin is estimated at 40–100 m, approximately 40–50 m in the Early Turonian, and as the transgression develops, up to 100 m in the second half of the Turonian. For the Coniacian time, the paleodepth of the basin is also estimated in the range of 40–100 m. This interval of the section corresponds to one eustatic cycle, the paleodepth was approximately 40–50 m in the Early Coniacian and, as the transgression developed, increased to 100 m in the second half of the Coniacian Age. In the Early Santonian, the paleodepth range did not exceed 100 m, and by the end of the Early Santonian it decreased even further. This range of the section corresponds to two eustatic cycles.

Six climatic cycles have been identified, beginning with the cooling phase. Relatively warmer epochs occurred at the end of the Early Turonian (19–22°C), the Late Turonian–early Coniacian (19–20°C) and three phases of warming in the early Santonian (19–22°C). Relatively colder epochs include the end of the Early Turonian and the Middle Turonian (18.5–19.5°C), the middle Coniacian–early Santonian (18.5–19°C), and three more episodes of cooling in the early Santonian (18.5–19°C).

Two intervals of relatively humid climate (Turonian–early Coniacian and the second half of Early Santonian, the time of member V formation) and an interval of arid climate (middle Coniacian–beginning of Early Santonian, the time of formation of the second half of submember IV-1 and submember IV-2) were identified.

Throughout the Turonian–Early Santonian time, the epicontinental sea basin that covered the area of the Voronezh anteclise was characterized by normal salinity, as evidenced by the finds of echinoderms, crustaceans, and pelecypods that lived in the Turonian–Coniacian time, as well as inocerami and cephalopods that lived here in the Early Santonian time. For the end of the Early Santonian, a local decrease in salinity (Sr/Ba ratio) was also noted, associated with a decrease in the basin depth.

FUNDING

This research was supported by the Interdisciplinary Scientific and Mathematical Methods for the Analysis of Complex Systems Educational School (Moscow State University), the Program of activities of the Rational Subsoil Use for 2019–2024 world-class scientific and educational center, with the support of the Ministry of Education and Science of Russia (order of the Russian Federation Government dated April 30, 2019 No. 537).

REFERENCES

Badulina, N.V., Yakovishina, E.V., Gabdullin, R.R., et al., Lithological-geochemical characteristics, and sedimentation conditions of Upper Cretaceous sections of Northern Peritethys, Byull. *Mosk. O–va Ispyt. Prir., Otd. Geol.*, 2016, no. 4-5, pp. 136–147.

O'Brian, C.L., Robinson, S.A., Pancost, R.D., et al., Cretaceous sea-surface temperature evolution: Constraints from TEX86 and planktonic foraminiferal oxygen isotopes, *Earth Sci. Rev.*, 2017, vol. 172, pp. 224–247.

Burgener, L., Hyland, E., Huntington, K.W., et al., Revisiting the equable climate problem during the Late Cretaceous greenhouse using paleosoil carbonate clumped isotope temperatures from the Campanian of the Western Interior Basin, USA, *Palaeogeogr., Palaeoclimat., Palaeoecol.*, 2019, vol. 516, pp. 244–267.

Engalychev, S.Yu. and Panova, E.G., Geochemistry and origin of sandstones of eastern part of Main Devonian Field in the north-west of Russian Plate, *Litosfera*, 2001, no. 5, pp. 16–29.

Gabdullin, R.R., *Ritmichnost' verkhnemelovykh otlozhenii Russkoi plity, Severo-Zapadnogo Kavkaza i Yugo-Zapadnogo Kryma* (Rhythmicity of Upper Cretaceous Deposits in the Russian Plate, Northwestern Caucasus, and Southwestern Crimea), Moscow: Mosk. Gos. Univ., 2002.

Gabdullin, R.R. and Ivanov, A.V., Rhythmicity of the carbonate sedimentation in the Late Cretaceous basin of the south part of the Voronezh Anteclise (on the example of the quarry of Stolenskyi mining-enriching factory), *Tr. NII Geol. SGU. Nov. Ser.*, 2002, vol. 10, pp. 41–55.

Gabdullin, R.R., Puzik, A.Yu., Merenkova, S.I., et al., Lithological and geochemical characteristics and paleoclimatic conditions of the formation of Upper Cretaceous sediments of the Russian Plate epicontinental basin in the region of the Ul'yanovsk–Saratov trough, *Moscow Univ. Geol. Bull.*, 2021, vo. 76, no. 3, pp. 257–269.

Climate in epochs of major biospheric reorganizations, in *Tr. GIN RAS, Vyp. 550* (Trans. Geol. Inst. Vol. 550), Semikhatov, M.A. and Chumakov N.M., Eds., Moscow: Nauka, 2004,

Merenkova, S.I., Seregina, I.F., Gabdullin, R.R., et al., Reconstruction of paleosalinity and bathymetry of Yenikale Strait in the Eastern Paratethys Ocean in Sarmatian: Evidence from geochemical data, *Moscow Univ. Geol. Bull.*, 2020, vol. 75, no. 4, pp. 342–352.

Teis, R.V. and Naidin, D.P., *Paleotermometriya i izotopnyi sostav kisloroda organogennykh karbonatov* (Paleothermometry and Oxygen Isotopic Composition in Organic Carbonates), Moscow: Nauka, 1973.

Transalted by M. Nickolsky